Dynamic identification of moisture sources in the Orinoco basin in equatorial South America

RAQUEL NIETO[1,2], DAVID GALLEGO[3], RICARDO TRIGO[2,4], PEDRO RIBERA[3] & LUIS GIMENO[1,2]

1 *Departamento de Física Aplicada, Facultad de Ciencias de Ourense, Universidad de Vigo, Campus As Lagoas s/n, ES-32004 Ourense, Spain*
l.gimeno@uvigo.es

2 *University of Lisbon, CGUL, IDL, Lisbon, Portugal*

3 *Departamento de Sistemas Físicos, Químicos y Naturales, Universidad Pablo de Olavide, Carretera de Utrera km.1, ES-41013 Sevilla, Spain*

4 *Universidade Lusófona, Departamento de Engenharias, Lisbon, Portugal*

Abstract The main areas of net moisture uptake are examined in air masses over the Orinoco River basin, located in equatorial South America, north of the Amazon basin. Although the Orinoco River has the third largest average annual discharge in the world (with 5.4×10^{11} m^3 year^{-1} draining into the Atlantic Ocean), the sources of moisture that feed it have not previously been studied in any detail. The results are presented from analyses of back-tracking of all the air masses over the Orinoco basin over a period of five years (2000–2004) using the diagnostic Lagrangian tool FLEXPART. The input data for the model were obtained from the European Centre for Medium-range Weather Forecasts (ECMWF). Air transported into the Orinoco basin experiences a large uptake of water over the tropical North Atlantic within the three days prior to its arrival over the basin. The Tropical South Atlantic and the eastern coast of the Pacific become significant moisture sources for about 5–10 days before arriving over the Orinoco basin. Contrary to what might be expected, large areas of the Amazon basin, along with the Gulf of Mexico, do not provide significant moisture to the study area. Interestingly, over these zones the air experiences net moisture loss. Preliminary analysis of the processes that occur leads to the conclusion that most of the water observed over the Orinoco basin derives from advective fluxes into the area, while recycling of moisture is negligible.

Key words Orinoco River; moisture sources; moisture transport; FLEXPART model

Identification dynamique des sources d'humidité dans le bassin de l'Orinoco en Amérique du sud équatoriale

Résumé Cette étude examine les principales zones de prise nette d'humidité dans les masses d'air au-dessus du bassin du Fleuve Orinoco, situé en Amérique du sud équatoriale, au nord du bassin de l'Amazone. Bien que le Fleuve Orinoco ait le troisième plus grand débit moyen annuel au monde (avec 5.4×10^{11} m^3 par an s'écoulant dans l'Océan Atlantique), les sources d'humidité qui l'alimentent n'ont pas encore été étudiées en détail. Nous présentons les résultats des analyses des rétro-trajectoires de toutes les masses d'air au-dessus du bassin de l'Orinoco pendant cinq ans (2000–2004) à l'aide de l'outil Lagrangien de diagnostic FLEXPART. Les données d'entrée pour le modèle ont été obtenues du Centre Européen de Prévision Météorologique à Moyen Terme (ECMWF). L'air transporté vers le bassin de l'Orinoco prélève une importante quantité d'eau au-dessus de l'Atlantique Nord Tropical durant les trois jours précédant son arrivée au-dessus du bassin. L'Atlantique Sud Tropical et la côte orientale du Pacifique deviennent des sources significatives d'humidité pendant environ 5–10 jours avant l'arrivée au-dessus du bassin de l'Orinoco. Au contraire de ce qui pourrait être prévu, de grands secteurs du bassin de l'Amazone, ainsi que le Golfe du Mexique, ne fournissent pas d'humidité significative au secteur d'étude. Il est intéressant de remarquer que l'air subit une perte d'humidité nette au dessus de ces zones. L'analyse préliminaire des processus en jeu mène à la conclusion que la majeure partie de l'eau observée au-dessus du bassin de l'Orinoco provient des flux advectés vers la zone, alors que le recyclage de l'humidité est négligeable.

Mots clefs Fleuve Orinoco; sources d'humidité; transport d'humidité; modèle FLEXPART

INTRODUCTION

In recent years, there has been a growing interest among the scientific community, particularly among meteorologists, climatologists and hydrologists, in the origin of the moisture and precipitation that occur over a given region. Given that water is essential for life, this is a topic of clear practical interest; it also addresses important scientific questions (Trenberth *et al*., 2003). However, the processes that determine the transport of atmospheric moisture are poorly understood. A firm understanding of the functional relationships involved is essential to guarantee

the sustainable development of many undeveloped regions in the world that may be prone to increased levels of water stress as a consequence of ongoing and future climate change (IPCC, 2007).

According to the latest IPCC assessment, increases in the concentration of greenhouse gases in the atmosphere could accentuate the hydrological cycle (IPCC, 2007) to a significant degree. An increase in evapotranspiration could, for example, add moisture to the atmosphere, which, if recycled, could directly increase rainfall and, simultaneously, increase latent heat release (associated with this increased rainfall), thus triggering intensified circulation patterns (e.g. the Hadley cell). These modifications could then change the patterns of moisture convergence from remote sources (Held & Soden, 2006). Hence, advances in understanding, and the ability to model and predict, the character of precipitation are vital, but require new approaches to examining data and modelling results. It is now commonly accepted that the precipitation that falls in a region has one of three origins (Brubaker *et al*., 1993): (a) moisture already present in the atmosphere, (b) moisture advected into the region by wind, or (c) evaporation from the surface below. This last term corresponds to the recycling component. While definitions can vary, recycling is commonly defined as that part of the evaporated water from a given area that contributes to precipitation over the same area (for a review, see Eltahir & Bras, 1996; Burde & Zangvil, 2001). Averaged over long periods, source (a) provides a negligible contribution. Therefore, two major processes are responsible for the observed atmospheric moisture: (i) local evaporation (recycling) and (ii) transport from remote sources (advection).

To quantify the relationship between the contributions of recycled and advected moisture is not straightforward. In general, most studies in this area require the use of sophisticated atmospheric models that determine the net moisture flows through the limits of the region under study (Chen *et al*., 1994; Fernandez *et al*., 2003; Liu & Stewart, 2003). Using these models, it is feasible to estimate the amount of moisture that arrives into a region from outside it (advection). It is possible to compute the amount of moisture that originates from within the region (i.e. the recycling component). The recycling rate thus obtained is a diagnostic measure of the potential for interactions between land surface hydrology and the regional climate. In a practical sense, the actual value of the recycling ratio is nevertheless considerably difficult to quantify. There are numerous methods for deriving this ratio. However, these are generally variations of the same set of mathematical equations, which depend on assumptions about the relationship between precipitable water and precipitation (Burde & Zangvil, 2001). Other approaches for estimating moisture recycling involve tracing water from its source region using forward modelling (Koster *et al*., 1986; Bosilovich & Schubert, 2002), back-trajectory modelling (Dirmeyer & Brubaker, 1999), or isotope observations (Wright *et al*., 2001).

The direct identification of these source regions may present several additional methodological complications. Traditionally, the origin of the moisture that feeds precipitation is identified by isotopic analysis or by using simple formulae for the balance of atmospheric moisture. The relationship between the relative proportions of certain isotopes of oxygen and hydrogen depends on the conditions (height, temperature or distance from the coast) under which the water evaporated to the atmosphere. As a result, it should be possible to establish an approximate relationship between the isotopic content of a sample and its origin (Rindsberger *et al*., 1983; Celle-Jeanton *et al*., 2001). Nevertheless, this method requires a precise knowledge of the study region, which may include undertaking repeated expensive sampling campaigns. Even then, results can be misleading as a consequence of the wide variety of sources from which sampling may take place.

The recent widespread use of powerful computers to analyse large databases, and weather data at a global scale, have allowed the development of new methods for assessing moisture sources, which are based on dynamic models of atmospheric transport. Models that account for source and sink regions of moisture in a Lagrangian framework range from simple analytical models (Dominguez *et al*., 2006) to numerical water vapour tracers (Joussame *et al*., 1984; Koster *et al*., 1986) and to algorithms that use quasi-isentropic back-trajectories in combination with model-

derived surface fluxes to determine evaporation sources along back-trajectories (Wernli, 1997; Massacand *et al*., 1998; Dirmeyer & Brubaker, 1999; Wernli *et al*., 2002).

Over the last decade, the Lagrangian dispersion model FLEXPART (Stohl *et al*., 1998) has permitted the propagation of different components of the atmosphere to be analysed. This model has been applied fundamentally to the analysis of pollutant dispersion at the continental (Rappenglueck *et al*., 2004) and intercontinental scales (Stohl *et al*., 2002). Recently, the accuracy and robustness of the model has been used to study moisture fluxes to locate the origin of extreme precipitation events (Stohl & James, 2004), and to assess average values for moisture sources (Stohl & James, 2005; Nieto *et al*., 2006, 2007).

The Orinoco River has the third largest river flow in the world, with a mean discharge of 5.4×10^{11} m^3 year^{-1} to the Atlantic Ocean. The Orinoco and Amazon rivers combined account for 25% of the freshwater discharge to the world's oceans. The Orinoco extends for nearly 2500 km and its associated drainage basin is the third largest in South America with an area of 830 000 km^2. About 77% of the drainage basin is in Venezuela, and the remainder in Colombia, between equatorial and tropical latitudes (and limited by the parallels 1°N and 11°N). The hydrographical network of the Orinoco is very extensive and is formed by lengthy and substantial tributaries. These tributaries convey high flows that reflect the abundant precipitation regime of the region. In mountainous regions, precipitation can easily reach 3000 mm year^{-1}, although values ranging between 1000 and 2000 mm year^{-1} are typical in the rest of the river basin (Silva León, 2005). The precipitation follows a seasonal cycle, with maxima occurring during the summer months as a consequence of the annual migration of the Intertropical Convergence Zone (ITCZ). At its mouth, the enormous volume of water from the Orinoco spreads out and forms a very large delta (Amacuro Delta) with a total surface area of about 22 500 km^2 and maximum width of 370 km. The Orinoco River basin contains a large variety of ecosystems, varying from prairies with a savannah climate to tropical and equatorial forests. Close to the delta, most ecosystems are aquatic in nature (Colonnello, 1996), flooding with seasonal increases in river flow (Colonnello, 2005).

Despite being one of the largest rivers in South America, few studies have been dedicated to evaluating the moisture sources that feed the Orinoco River network. In contrast, there is relatively extensive literature on the same subject that covers the neighbouring Amazon basin. Since the 1990s, important large-scale experiments have been implemented using data from flux towers and from more comprehensive data sets using streamflow, rainfall and upper air information. Moreover, the recycling ratio has been the subject of studies since the mid-1970s (e.g. Molion, 1975; Salati & Marques, 1984). Moisture transport in and out of the Amazon basin has also been studied using a variety of data sets varying from radiosondes to global reanalyses, as well as from climate model simulations (reviews in Costa & Foley, 1999; Marengo & Nobre, 2001; Marengo, 2005, 2006; and references quoted therein). These authors have estimated the hydrological cycle, its variability, and the effects of both remote atmospheric impacts and local forcing on the variability of the components of the water balance, as well as the closure of the water balance for the whole of Amazonia. However, most of the studies on the Orinoco River basin are included within general-purpose climatologies (Labraga *et al*., 2000).

The main objective of the study reported herein was to apply the new Lagrangian diagnosis model used by Stohl & James (2004, 2005) to identify the main moisture sources for the Orinoco River basin. To achieve this, we tracked the air masses backwards, in order to establish where the air gains or loses moisture. It is important to stress that in the study we identified those regions where the air acquired water vapour when it crossed over them.

METHOD

In order to determine the origin of the moisture over the Orinoco River basin, we based our study on the Lagrangian particle dispersion model FLEXPART developed by Stohl *et al*. (1998) and recently adapted to detect moisture sources (Stohl & James, 2004, 2005). Recently, the authors

have also adopted this method to evaluate the moisture sources associated with the Sahel (Nieto *et al*., 2006) and Iceland (Nieto *et al*., 2007). FLEXPART runs using data from the objective analysis from the European Centre for Medium-range Weather Forecasts (ECMWF, 2002) to track atmospheric moisture along trajectories. The atmosphere is divided homogeneously into a large number of so-called particles. The particles are distributed homogeneously in the atmosphere according to the distribution of atmospheric mass. These particles are then advected by the model using operational three-dimensional (3-D) ECMWF winds. As they move, the particles' mass remains constant. To calculate both the grid-scale advection as well as the turbulent and convective transport of particles, operational ECMWF data were also input to the model. Their positions and their specific humidity data (q) were interpolated from the ECMWF data being recorded every 6 h. Increases (e) and decreases (p) in moisture along the trajectory can be calculated with the FLEXPART model through changes in q with time, $e - p = m \cdot (\mathrm{d}q/\mathrm{d}t)$, where m represents the mass of the particle. By summing $e - p$ for all the particles in the atmospheric column over a given area, we can obtain $E - P$, the surface freshwater flux, where E is the evaporation and P the precipitation rate per unit area. In a Lagrangian framework, air-parcel back-trajectories can provide a link between the evaporative sources of water vapour and the precipitation elsewhere.

The method can also track $E - P$ from a region backwards in time by evaluating the $e - p$ values along the trajectories, choosing the appropriate particles to find regions where those particles have either gained or lost moisture. The E – P values can be calculated for a certain point backwards in time, or can be integrated over a certain period backwards from when the target criteria were fulfilled. It should be noted that throughout this paper we define "moisture source region" as an area in which an air parcel has either absorbed or expelled significant amounts of moisture before reaching the Orinoco River basin.

The FLEXPART model (Stohl *et al*., 1998) uses ECMWF operational analysis every 6 h with a 1° × 1° resolution on 60 vertical levels. The level density is higher at lower levels, with approximately 14 model levels below 1500 m and 23 levels below 5000 m. To ensure exact mass balance, vertical winds are calculated using spherical harmonics data as part of the data-retrieval procedures at ECMWF. In order to account for turbulence, the FLEXPART model calculates the trajectory of the particles using random oscillations superimposed on analysed winds. In the planetary boundary layer (PBL), these random oscillations are calculated by solving the Langevin equations for Gaussian turbulence (Stohl & Thompson, 1999). These equations use Lagrangian time scales and the standard deviations of the wind components, which are computed from ECMWF PBL parameters (Hanna, 1982). The PBL height is determined using a combined Richardson number and lifting parcel technique (Vogelezang & Holtslag, 1996), while, outside the PBL, turbulence is assumed to be very small. Given a sufficiently large area of atmospheric column, instantaneous effects of turbulence and convection on column-integrated properties can be neglected. Although global data sets cannot provide sufficient resolution to determine the characteristics of individual convective cells, they can nevertheless reproduce the large-scale effects of convection, particularly humidity variations (Stohl & James, 2005). The FLEXPART model has a number of options for simulating particle generation. In this case, the atmosphere was "filled" homogeneously with particles, each representing a fraction of the total atmospheric mass. Particles were then allowed to move freely (forwards in time, but this is arbitrary) with the winds for the duration of the simulation. This method has limitations, mainly relating to the accuracy of the trajectory and the fact that it uses a time derivative of humidity (unrealistic fluctuations in humidity could be considered as moisture fluxes). Although it is acknowledged that such types of error may play an important role when evaluating the trajectories of individual particles, the use of large time periods, as well as large spatial averages minimises overall gross error significantly. Stohl & James (2004, 2005) provide the complete mathematical formulation of the method and describe how the climatologies are calculated. Here we give a qualitative description of the method, and refer the reader to those previous papers for details.

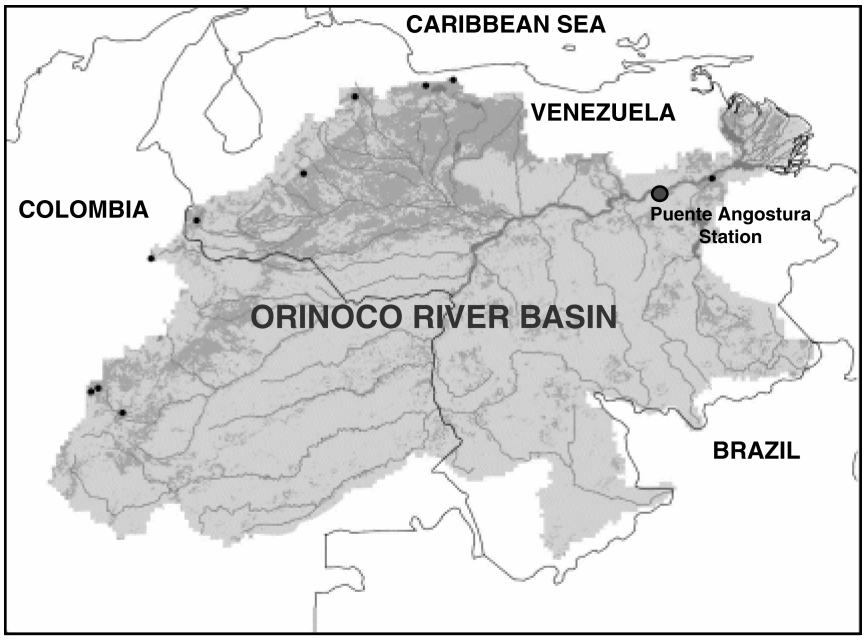

Fig. 1 Map of the Orinoco River basin (grey area) showing the position of Puente Angostura station (8.14°N; 63.6°W) (large dot), having the longest and most complete time series of discharge data for the Orinoco basin.

The study region (Orinoco River basin, Fig. 1) was translated into a grid of 1° latitude × 1° longitude that encloses the entire river basin. The particles considered in the moisture transport model correspond to those that arrive, at a given instant, at one of the grid-points identified in this region. Here, we considered the trajectories of 1 398 801 particles of equal mass for the 5-year period between 1 January 2000 and 31 December 2004. Instead of representing individual trajectories, the specific moisture variations were spatially averaged over the same grid network and for different periods (1–10 days in advance), with results being averaged at the daily scale. Consequently, the representation of $E - P$ for Day 1 indicates the regions where the particles (that will arrive on the following day at some point in the Orinoco River basin) have lost or gained moisture. Similarly, the $E - P$ pattern for Day 2 indicates the regions where the particles lose or gain moisture two days before they arrive at the river basin. The procedure was repeated for each day, up to and including Day 10. Although the average residence time of water in the atmosphere is different for various locations on the Earth, and the residence time varies from case to case, we assumed a value of 10 days, because this is the average time that water vapour resides in the atmosphere (Numaguti, 1999). Representation on a daily basis allows the geographic location of the moisture sources, and the moment at which these sources become significant for the study region, to be identified.

RESULTS

Figure 2 shows the annual averages of $E - P$ for the period 2000–2004 for all the air masses that end up over the Orinoco River basin. Despite the relative complexity of the back-tracking method, the interpretation of these patterns should be fairly simple, providing a good representation of moisture source and sink regions. In order to facilitate their interpretation, results corresponding to regions characterised by $E - P > 0$ (Fig. 2, right column) and $E - P < 0$ (Fig. 2, left column) are represented separately. In the first case, evaporation dominates over precipitation, which indicates that air particles located within that vertical column (and bound to reach the river basin of the Orinoco) gain moisture. These regions are therefore identified as moisture source regions. In contrast, maps that represent $E - P < 0$ reveal regions where precipitation dominates over

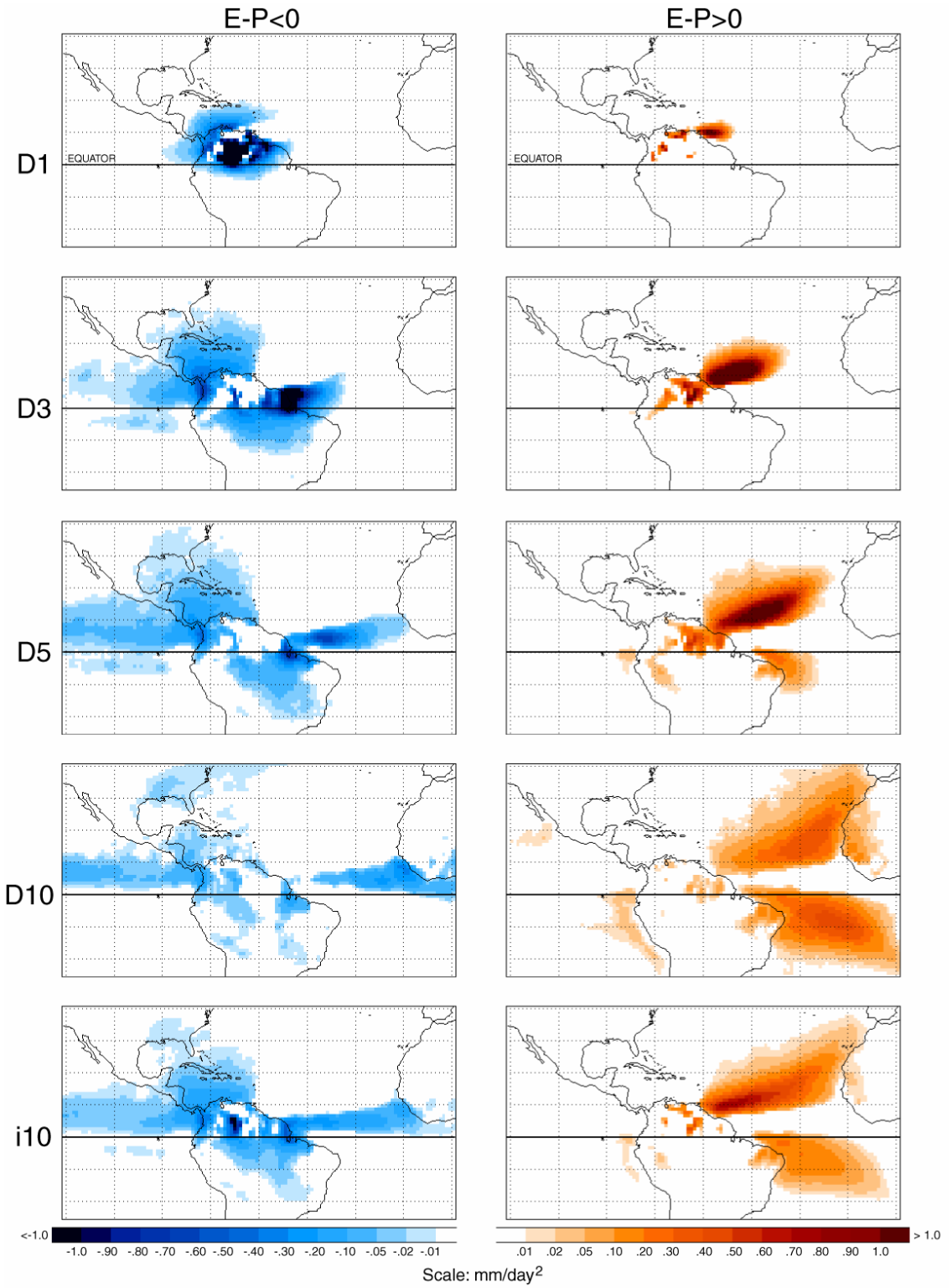

Fig. 2 Annual average values of $E - P$ (period 2000–2004) for all the particles bound for the Orinoco River basin. Right and left columns show, respectively, source and sink regions that are characterised by positive / negative values of $E - P$ for days 1 (D1), 3 (D3), 5 (D5) and 10 (D10). Aggregated values for the first 10 days are shown in the bottom panel (i10).

evaporation. Consequently, air masses located over these regions in transit to the Orinoco River basin display a net loss of moisture, and these regions are identified as moisture sink regions. It should be stressed that the results shown in Fig. 2 represent temporal averages for a period of 5 years with a time-step resolution of 6 h. Thus, each point of the mesh represents the aggregated average for a large number of individual particles. In consequence Fig. 2 should be interpreted strictly from a climatologic point of view. For example, a grid-point that shows a positive value (i.e. $E - P > 0$) indicates that, on average, most of the particles (not necessarily all) that pass through the grid point (and that have the Orinoco River basin as their final destination) gain moisture.

Annual average values of positive and negative $E - P$ were computed for the preceding 10 days, from Day 1 until Day 10. For the sake of clarity, we show results restricted to days 1, 3, 5 and 10 (hereafter D1, D3, D5 and D10) respectively. Thus, the D1 map indicates those regions on which the air masses gain ($E - P > 0$) or lose ($E - P < 0$) moisture during the day before their arrival in the Orinoco basin. This temporal proximity limits the spatial extent of the influence of those zones that are near their destination area. It is during this first day that the process of recycling is most relevant, when air masses are loaded with moisture from the same region into which they will soon fall as precipitation. In the case of the Orinoco River basin (see Fig. 2, D1) the air masses gain moisture only during the previous day. For D1, the air is already starting to lose moisture, as is indicated by the shading over the river basin and its proximities (as shown for the $E - P < 0$ pattern), which indicates that the recycling process is of little importance in the Orinoco River basin.

Spatial patterns relative to D3, D5, and D10 show the source and sink regions of moisture for those particles that will reach the Orinoco basin within three, five, and 10 days, respectively. As we move back in time, the spatial extent of those source and sink regions of particles is expanded, and generally less intense, i.e. they become more diffuse. This result may reflect two different phenomena: (a) increasing dispersion of particles, and (b) gain or loss of moisture over periods longer than five days for successive processes in their trajectory. When average values are calculated for large numbers of particles, random values tend to cancel each other out, except in those zones that contribute to trajectories that are mostly in the same "direction". The results shown in Fig. 2 indicate the existence, at the annual scale, of three preferred moisture source regions for the Orinoco basin. Apart from the recycling process described above observed patterns of $E - P > 0$ for D1 and D3 show that, in the short term, the Tropical North Atlantic is the main region of moisture source in this river basin (hereafter called TNAS). This source also reflects the prevailing wind direction in that tropical region and the steep orography close to the Atlantic coast in the eastern section of the river basin. The spatial pattern for D5 begins to reveal the existence of a source region located in the tropical South Atlantic (hereafter called TSAS). The relevance of this region increases for D10, when it becomes as important as the corresponding source region located in the northern hemisphere. Finally, the D10 map shows a smaller third oceanic source region located in the eastern coast of the Pacific, close to Peru and the Equator.

In the following section, we show that these source regions are supported by regional atmospheric circulation and that values of $E - P$ are linked to runoff and precipitation values computed for the Orinoco basin.

The corresponding analysis for sink regions highlights those sectors that are characterised by negative values of $E - P$ (left column of Fig. 2). The pattern for one day in advance (D1) indicates that the most important characteristic is the intense loss of moisture over the river basin. This result indicates that, on average, a large percentage of air particles were already over the river basin on the previous day, and in general, are already losing the moisture they had previously gained further away. As we go further back in time (D3), it can be seen that the majority of particles passing over the Gulf of Mexico and the Amazon (on their way to the Orinoco basin) lose large amounts of moisture. The equatorial band that stretches from the eastern Pacific to the western Atlantic becomes an important sink source when the patterns for D5 and D10 are taken into account. This result was predictable, because those particles that cross the ITCZ on their

trajectory lose a large amount of their moisture (independently of being over the Pacific or the Atlantic oceans).

Finally, the two maps at the bottom of Fig. 2 correspond to the integrated behaviour of particles from Day 1 to Day 10 (identified as i10). These maps show the average of all the gains and losses of moisture for the 10 previous days. From this aggregated perspective, it is confirmed that the two most important regions acting as moisture source are located on the southern and northern tropical sectors of the Atlantic (TNAS and TSAS), whereas the three main sinks sources are located at: (a) the equatorial band, (b) the Amazon River basin, and (c) the Gulf of Mexico.

The seasonal variability of patterns obtained is shown in Fig. 3. Figure 3 shows the average values obtained for the 10 days for the wet season (JJAS) and the dry season (DJFM). In general, the geographic locations of the main source (Fig. 3, right column) and sink (Fig. 3, left column) regions do not vary significantly throughout the year. However, important variations are seen in both the latitudinal extent and the relative magnitude of these sources. The source regions ($E - P > 0$) increase their moisture contribution during the corresponding hemisphere's winter. Thus, the role of the tropical North Atlantic as a moisture source increases between December and March, and presents a relative minimum between June and September. On a smaller scale, the TSAS displays a maximum between June and September and almost vanishes as a source region between December and March. The seasonal variability of sink regions ($E - P < 0$) over the equatorial Atlantic closely follows the corresponding seasonal migration of the ITCZ. Thus, during the period between June and September, this sink region is displaced to the north of the Equator, whereas between December and March it is located further south, closer to the Equator. However, as previously stated, these variations are relatively minor. The equatorial Pacific region acts as an important sink during the dry season (DJFM) and practically disappears in the wet season (JJAS). The sink sector located in the Caribbean Sea maintains a similar intensity throughout the year. In contrast, the sink sector over the Amazon basin displays important seasonal changes in intensity, probably related to variations in incoming solar irradiation. Thus, the extent of this region is limited between April and September. Between October and March, however, this region

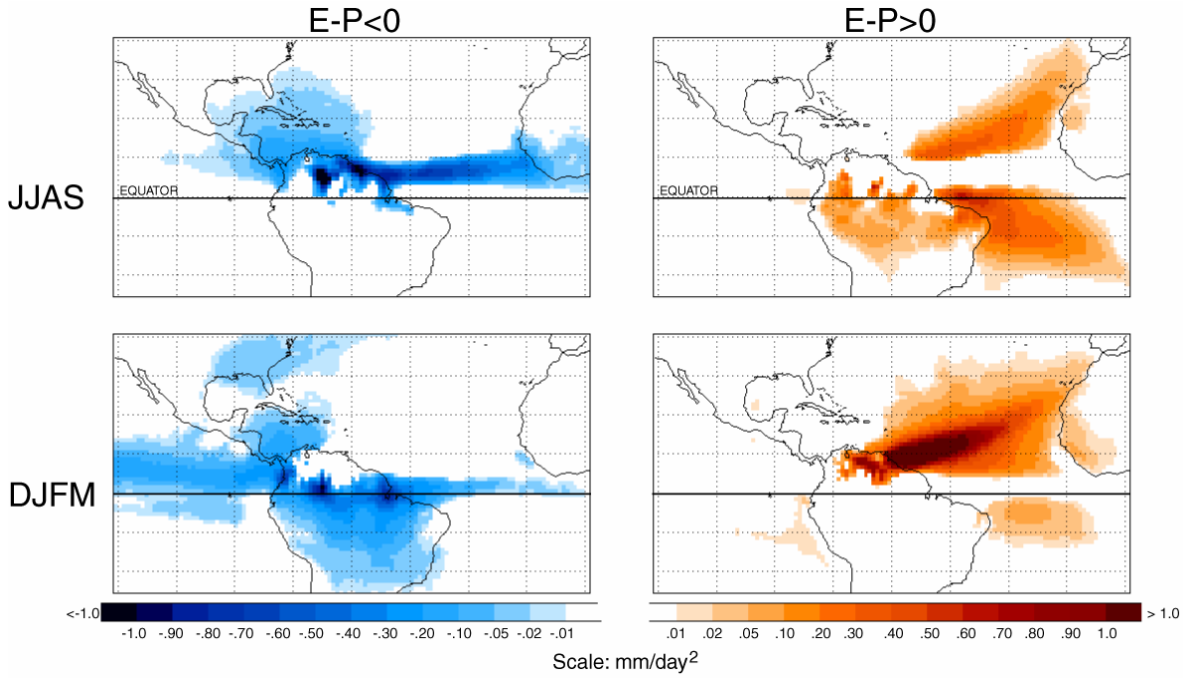

Fig. 3 Seasonally averaged values of $E - P$ (period 2000–2004) for all the particles bound for the Orinoco River basin. Only the aggregated values for the first 10 days are shown (i10) in a similar way as the bottom panel in Fig. 2.

extends much further south, occupying a large percentage of the entire South American continent. During this season, there is extreme aridity over the Amazon basin due to the thermal inversion that accompanies the trade winds during this period. Finally, the Pacific sink region is also characterised by an increase in its intensity between the wet season, being restricted to the South America coastal area, and the dry season, when it extends throughout the eastern and central Pacific (mostly to the north of the Equator).

METEOROLOGICAL BASIS AND HYDROLOGICAL IMPLICATIONS

We now show that the results for the moisture sources obtained in the previous section are in agreement with existing data for the large-scale atmospheric fluxes that affect the Orinoco region. To demonstrate this, we used the stream functions as parameters of two-dimensional, non-divergent flows, with values that are constant along each streamline. Figure 4 shows the monthly long-term mean (1968–1996) of stream functions derived from NCAR/NCEP reanalysis (National Center for Atmospheric Research/National Centers for Environmental Prediction; Kalnay *et al*., 1996) for wet and dry seasons (left and right, respectively). The stream function data are given in a Gaussian grid with longitudinal (latitudinal) resolution of 1.875° (2°), for a near-surface altitude (sigma level of 0.995) for the spatial window delimited by 20°N–8.571°S and 90°W–20.63°W.

The zero isoline delimits the frontier of the flux characterised by positive (negative) values, which indicates a clockwise (anticlockwise) vorticity. During the dry season (Fig. 4, bottom panel) the zero isoline is located over, or to the south of, the Orinoco basin, in such a way that the trajectories arriving at the Orinoco basin originate mainly from the tropical North Atlantic Ocean (thick arrow in Fig. 4). Therefore, for this case, the main source of moisture is the TNAS, whereas the contribution of the TSAS to the Orinoco basin moisture is considerably smaller. However, during the wet season (Fig. 4, top panel), the zero isoline is displaced to the north along the northern limit of the Orinoco basin and the fluxes from the North Atlantic do not affect the Orinoco basin with the same intensity. Under this configuration, the TSAS becomes more important, and both sources have a comparable contribution. This seasonal variation in the relative importance of the two main sources is in clear agreement with the meridional seasonal migration of the ITCZ (Alpert, 1945; Hastenrath, 1966, 2002; Poveda *et al*., 2006). The migration of the ITCZ is the main factor dominating the annual hydro-climatic cycle over the intertropical regions of South America and southern Mesoamerica (Poveda *et al*., 2006), because the ITCZ controls the various dynamics of the trade winds over oceans and land masses.

In order to assess the potential implications of our Lagrangian results of $E - P$ for the hydrological cycle of the Orinoco River basin, we evaluated the impact of monthly $E - P$ values obtained for the two major source regions of moisture (TNAS and TSAS) on the corresponding monthly precipitation and runoff series over the Orinoco basin. However, due to the limited availability of data, we were only able to explore the temporal variability of these four time series for the period from January 2000 to December 2004. These series were calculated as follows:

(a) The $E - P$ monthly time series was computed on the basis of the i10 $E - P$ values (i.e. the integrated values from D1 to D10) for both main moisture sources. The index was calculated as the sum of the values of i10 $E - P$ (initially calculated on a grid of 1° resolution) for the two boxes defined over the identified source areas. The TNAS box was defined between 7–17°N and 60–30°W, while the TSAS was defined between 2°N–7°S and 45–22°W (Fig. 5).

(b) The monthly mean precipitation index was computed using data from the Global Precipitation Climatology Project Version 2 data set (GPCP; Huffman *et al*., 2001; Adler *et al*., 2003). The GPCP is a merged dataset, on a 2.5°-resolution global grid, that merges information from rain gauge observations, satellite retrievals and sounding observations. The index was calculated in a box over the Orinoco River basin, defined between 10.5–2.5°N and 72.5–61.5°W (Fig. 5), and restricted to grid points located over the continent.

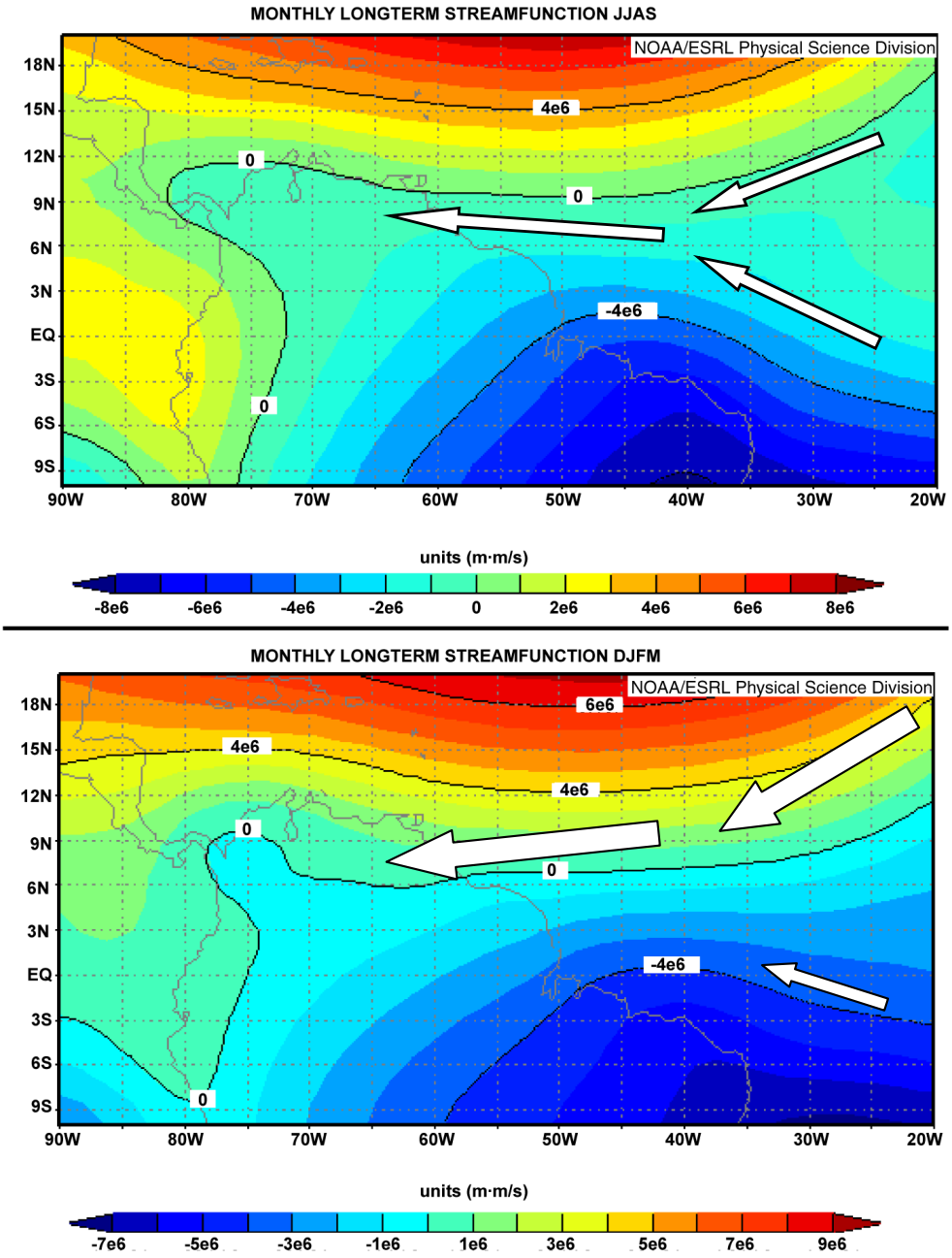

Fig. 4 Monthly long-term means (1968–1996) of stream function (mm s^{-1}) over the Orinoco River area for the wet season (June–September; top panel) and dry season (December–March; bottom panel). Arrows represent qualitatively the strength of the two main moisture source regions associated with the main atmospheric fluxes reaching the Orinoco basin.

(c) The monthly mean surface runoff index was calculated on the basis of data from the Climate Diagnostics Center (CDC) Derived NCEP Reanalysis II Products AC (Kistler *et al.*, 2001). The surface runoff data are given in a Gaussian grid with longitudinal resolution of 1.875° and a latitudinal resolution about 2°. The runoff index was calculated for the same box as was defined above for the precipitation index (Fig. 5).

Figure 6 shows the temporal variability of the four monthly time series described above. Columns in black represent the Orinoco basin runoff index, the blue line represents the precipitation index

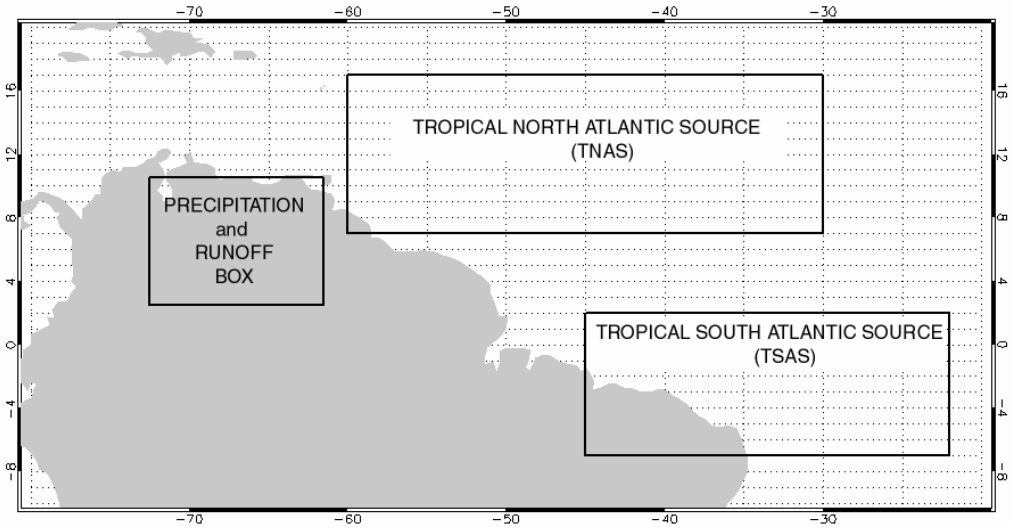

Fig. 5 Boxes where monthly indices used in Fig. 6 were calculated.

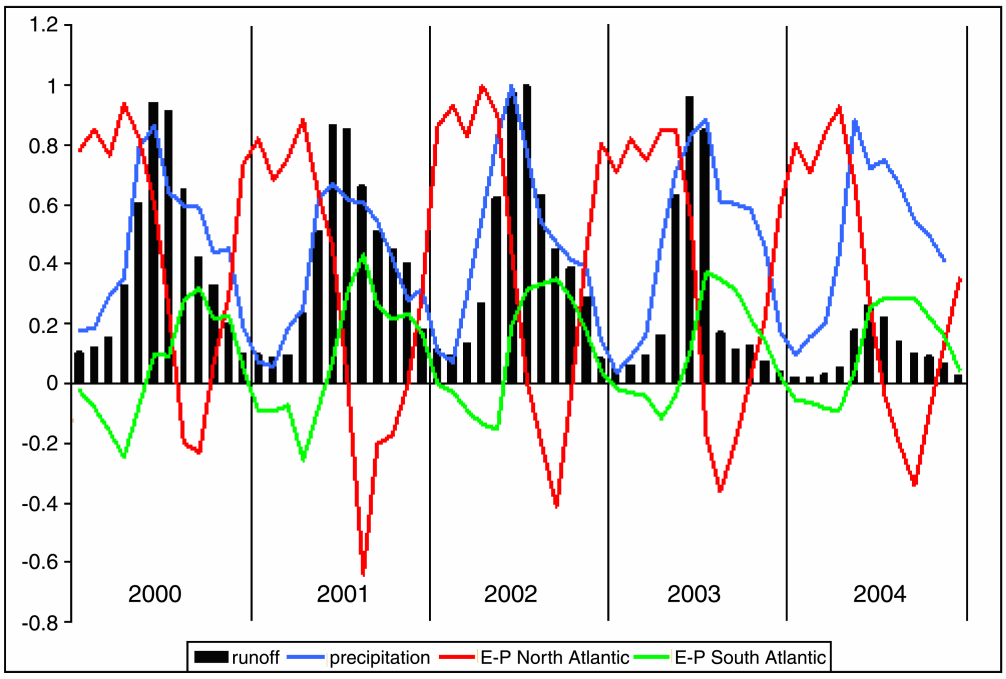

Fig. 6 Scaled monthly values (2000–2004) of runoff (black columns, in kg d^{-1} m^{-2}), precipitation (blue line, in mm d^{-1}) and i10 $E - P$ (evaporation minus precipitation integrated for the 10 previous days, in mm d^{-2}) obtained over the TNAS (red line) and TSAS (green line) boxes.

over the basin, and the red and green lines represent the $E - P$ indices defined over the TNAS and TSAS, respectively. All time series were scaled in order to facilitate meaningful comparison among them. The runoff and precipitation values were divided by the corresponding absolute maximum of each series, while the two $E - P$ time series were divided by the absolute maximum of either series. Precipitation over the basin shows a unimodal annual cycle that peaks in June–July, sometimes with a quasi-plateau structure that occurs during August–October, while the minimum occurs from December to March. These results are in agreement with those obtained by Poveda *et al*. (2006), showing that for the Orinoco basin, rainfall is governed by the seasonal migration of the ITCZ. The runoff series shows similar seasonal behaviour, with maximum values

occurring from June to October, and with minimum values from December to March. Both precipitation and runoff series are characterised by curves of distinct steeply rising and moderately decreasing slope. The annual evolution of the $E - P$ series shows again the different contributions over the Orinoco River basin of the TNAS and TSAS sources throughout the year. Both series show some out-of-phase behaviour, with the TNAS contribution peaking around April and May, one to two months before the maximum precipitation and runoff, while the TSAS has a maximum contribution around August–September, coincident with the quasi-plateau structure of precipitation and runoff. These results show that significant amounts of moisture from the TNAS are necessary to "start" the annual cycle of precipitation and runoff over the river basin, before the maxima of these two variables is reached. After this, there is a gradual reduction in precipitation until August, although the trend is less clear and an upturn may even occur during the following months. The quasi-plateau structure coincides with the maximum contribution of $E - P$ from the TSAS box. In summary, we believe that both sources of moisture play an important role in determining the precipitation and runoff regimes observed in the Orinoco River basin. The TNAS starts to provide large amounts of moisture at the beginning of the year. However, this is not converted into precipitation either throughout the winter or in the following early spring. This inefficiency in transforming moisture into rainfall is related to the lack of dynamic instability associated with the surface convergence linked to the ITCZ to the south of the Orinoco basin. In fact, the TNAS only starts to provide moisture more efficiently for precipitation during late spring and early summer. In contrast, moisture that arises from the TSAS appears to be used more efficiently (its seasonal cycle being more in phase with the precipitation/runoff) providing moderate values of precipitation during late summer and autumn, therefore feeding the runoff in the Orinoco basin. This behaviour fits in well with known ITCZ migration behaviour that permits the TSAS to gain in importance when the ITCZ is displaced northwards.

Further evidence of these hydrological implications can be derived from a study of the relationships between the discharge of the Orinoco River and the magnitude of $E - P$ obtained for the main source of moisture (TNAS). The longest and most complete time series of discharge data for the Orinoco basin corresponds to the Puente Angostura station, located near the mouth of the main river channel (latitude: 8.14°N, longitude: 63.6°W) before it dissipates into the Orinoco coastal delta (Fig. 1). Unfortunately, a mismatch in the availability of data makes this task rather difficult. The time series for the river flow from Puente Angostura ends in 1989, and reliable reanalysis data for the open ocean is possible only after widespread use of satellite data in 1979 (Kalnay *et al*., 1996). Therefore, the time during which comparison is possible is limited to the 11-year overlapping period, 1979–1989. Furthermore, given that the analysed period is prior to our $E - P$ Lagrangian data (2000–2004), we used $E - P$ data calculated through an Eulerian model by Trenberth & Guillemot (1998). These $E - P$ Eulerian values represent the net flesh flux water over a selected area. The $E - P$ values were taken from the on-line analysis by Trenberth & Stepaniak (http://www.cgd.ucar.edu/cas/catalog/newbudgets/index.html#Sec7), who used NCAR/NCEP data. These values were extracted with a grid resolution of 2.81° longitude × 2.79° latitude. The Eulerian $E - P$ index was calculated as the sum of the $E - P$ values of the grid points included in the TNAS box. We assessed the best seasonal link between the TNAS and river discharge comprehensively, with particular emphasis on the summer because this corresponds to the peak river flow season. The best results were obtained when applying a two-month lag, between the spring (April–June) average of Eulerian $E - P$ in TNAS, and the corresponding summer (June–August) average of river discharge in Puente Angostura. The annual cycles of these two quantities were normalised to facilitate the comparison (Fig. 7). Good visual agreement between the two series was confirmed by computation of the Pearson correlation coefficient ($R = 0.74$, statistically significant at the 1% significance level, with $N = 11$), which confirms the importance of the link between this moisture source box and the hydrological cycle in the Orinoco basin.

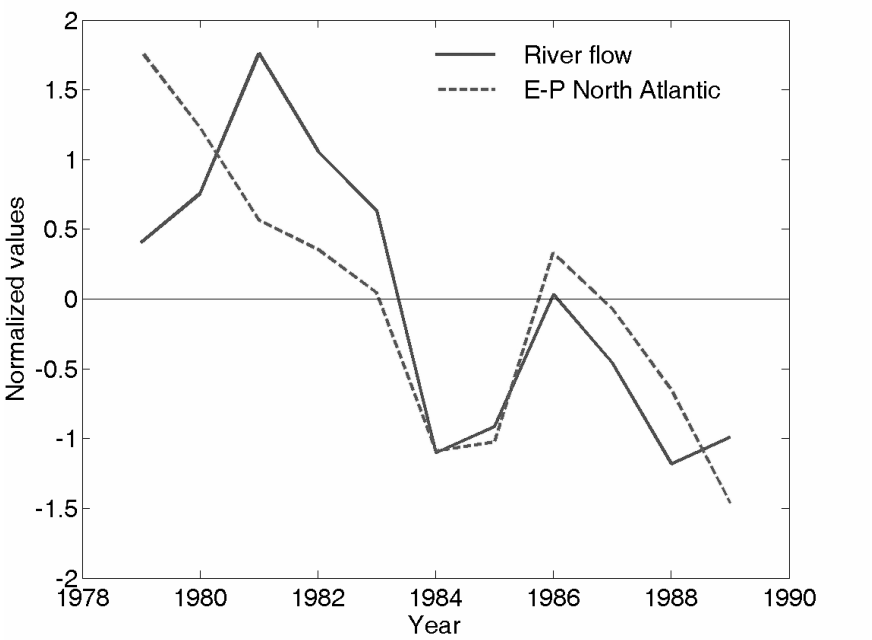

Fig. 7 Normalised spring (average April–June) series of Eulerian $E - P$ for the TNAS (solid line; mm d^{-1}) box and the corresponding summer (average June–August) of discharge in Puente Angostura (dotted line; $m^3 s^{-1}$).

CONCLUSIONS AND DISCUSSION

We used a robust and recently-developed dynamic 3-D back-tracking algorithm to assess the location and relative importance of moisture sources for the Orinoco River basin. We studied the average conditions over a 5-year period (2000–2004), which can be considered a standard period at the global climate scale, because there were no extremes of major modes of climate variability such as ENSO (El Niño-Southern Oscillation) or NAO (North Atlantic Oscillation). It should be stressed that the concept of net uptake of moisture source in this work is restricted by the capacity of the Lagrangian model to track those regions where an air parcel has either absorbed or expelled water before reaching the Orinoco River basin. The main results can be summarised as follows:

– The most important moisture source regions that affect the Orinoco River basin are (in decreasing order): the tropical North Atlantic, the tropical South Atlantic and finally, to a lesser extent but still detectable, the eastern coast of the Pacific Ocean. The tropical North Atlantic provides large amounts of moisture throughout the year. However, its greatest contribution occurs from January to June. The maximum moisture contribution that comes from the south tropical region can be observed from July to September. These results show that the relative importance of the source region depends on the preferred trajectories of the air masses to a greater extent than on skin temperatures (i.e. the potential evapotranspiration). During each hemisphere's winter, the trade winds are more intense and constant, this being one of the main factors that influence moisture transport.

– The most important sink zones were shown to be located in the Gulf of Mexico, the Amazon basin, and the long equatorial band that includes both the Pacific and the Atlantic. Traditionally, the Amazonian region and the Gulf of Mexico have been considered moisture sources by virtue of their capacity to evaporate large quantities of water. However, our results show that these regions do not provide moisture to the Orinoco River basin in equal measure from every direction, and a large percentage of the moisture generated in these regions never arrives at the river basin. This result indicates that, on average, air masses that cross the Amazon or the Gulf of Mexico on their way towards the Orinoco lose a large part of their moisture before arriving at Colombia or Venezuela.

These results indicate that advection of moisture is the fundamental process that contributes to moisture in the study region. Therefore, we conclude that recycling does not contribute appreciably. This result is considerably different to that of similar studies developed for high (Nieto *et al*., 2007) and subtropical (Nieto *et al*., 2006) latitudes where recycling was shown to be the main moisture source.

Finally, from a hydrological point of view, we may conclude that the main sources of moisture detected with our approach present a clear link with the precipitation and runoff observed in the Orinoco River basin, albeit with different seasonal contributions. The tropical North Atlantic source affects and modulates the precipitation during late spring and early summer, while the subtropical South Atlantic source maintains it during late summer and autumn, feeding the runoff and maintaining the water contribution into the basin. Maximum values of moisture over the tropical North Atlantic source have implications for the discharge of the Orinoco River, with the highest level of the relationship being obtained for a lag of two months after the beginning of the wet season.

The study reported herein shows the capacity of this dynamic method to locate the origin of the moisture that arrives in a given region. This approach is able to quantify the relative importance of each of these source (or sink) regions. Moreover, similarly to previous applications (Nieto *et al*., 2006, 2007) it is possible to evaluate the relative contribution of the two most important processes: advection and recycling.

The Lagrangian model that we used focuses on analysing moisture sources and sinks from a climatological perspective. However, it is also possible to apply this approach to individual extreme precipitation events, such as the catastrophic episode (floods) that took place in December 1999 in Venezuela. Fifteen days of constant and intense torrential rainfall culminated, on 16 December 1999, in extensive flooding and massive landslides in seven northern states of the country, including the urban area of the Venezuelan capital, Caracas. The effects were described as the country's worst natural disaster in modern history, with an estimated death toll of 20 000–30 000 people (USAID, 2000). The total cost of damages for the national government was estimated at about US$15 $\times$ 10^9 and approx. 600 000 people were directly affected. We believe that it is important to apply (with some adaptations) the method described in this paper to evaluate the moisture sources for this extreme event. This approach, together with a full characterisation of the weather patterns for those days, will permit evaluation of the relative importance of different moisture sources (such as abnormal high sea-surface temperature (SST) values in one or more regions identified in the present work). In particular, the correct identification of these moisture sources in December 1999 may be used in forecasting models that aim to predict the appearance of conditions that favour the occurrence of such extreme events.

Finally, we believe that this method points towards interesting perspectives on future investigations of the impact of climate change on water resources. Different climate change scenarios predict slightly different increases in global average temperatures. However, these scenarios also predict an intensification of the water cycle (IPCC, 2007) as a consequence of the larger capacity for evaporation and transport of warm air. Nevertheless, the results obtained here suggest that over certain regions, it is probably more important to evaluate changes in the magnitude and/or frequency of particular atmospheric circulation patterns. For the Orinoco River basin, any disturbance in the regime of trade winds would have important consequences for the precipitation. Naturally, the precise evaluation of these types of results requires the application of similar Lagrangian models to the output of the next generation of GCMs (global climate models), forced with updated climatic change scenarios. These models are currently being developed and it is expected that they will provide quantifications of the impact of the climate change on moisture transport in the near future.

Acknowledgements We thank Andreas Stohl for providing the trajectory data. Raquel Nieto thanks the “Fundação para a Ciência e a Tecnologia” (FCT) of the Portuguese Ministry of Science

(SFRH/BPD/22178/2005). The work was partially funded through the "Ministerio de Educación y Ciencia" (MEC) grant "DINPRE" (CGL2004-05187-C03-02/CLI). We would also like to thank the two anonymous reviewers for their helpful and constructive comments. The Eulerian $E - P$ values were taken from http://www.cgd.ucar.edu/cas/catalog/newbudgets/index.html#Sec7 by Trenberth &Stepaniak. Figure 4 was adapted from those provided by the NOAA-CIRES Climate Diagnostics Center, Boulder, Colorado, from their web site at http://www.cdc.noaa.gov/.

REFERENCES

Adler, R. F., Huffman, G. J., Chang, A., Ferraro, R., Xie, P., Janowiak, J., Rudolf, B., Schneider, U., Curtis, S., Bolvin, D., Gruber, A., Susskind, A. & Arkin, P. (2003) The Version 2 Global Precipitation Climatology Project (GPCP) monthly precipitation analysis (1979−present). *J. Hydromet*. **4**, 1147−1167.

Alpert, L. (1945) The intertropical convergence zone of the eastern Pacific region. *Bull. Am. Met. Soc.* **26**, 426–432.

Bosilovich, M. G. & Schubert, S. D. (2002) Water vapour tracers as diagnostics of the regional hydrologic cycle. *J. Hydromet.* **3**, 149–165.

Brubaker, K. L., Entekhabi, A. & Eagleson, P. S. (1993) Estimation of continental precipitation recycling. *J. Climate* **6**, 1077−1089.

Burde G. I. & Zangvil, A. (2001) The estimation of regional precipitation recycling part one: review of recycling models. *J. Climate* **14**, 2497−2508.

Celle-Jeanton, H., Travi, Y. & Blavoux, B. (2001) Isotopic typology of the precipitation in the western Mediterranean region at three different time scales. *Geophys. Res. Lett.* **28**, 1215−1218.

Chen, T. C., Pfaendtner, J. & Weng, S. P. (1994) Aspects of the hydrological cycle of the ocean−atmosphere system. *J. Phys. Ocean.* **24**, 1827−1833.

Colonnello, G. (1996) Aquatic vegetation of the Orinoco River Delta (Venezuela). An overview. *Hidrobiología* **340**, 109−113.

Colonnello, G. (2005) Clave ilustrada de gramíneas acuáticas del Delta del Río Orinoco y aspectos de su ecología (Venezuela). In: *Humedales de Iberoamérica, experiencias de estudio y gestión*. Red Iberoamericana de Ciencia y Tecnología para el Desarrollo.

Costa, M. H. & Foley, J. A. (1999) Trends in the hydrologic cycle of the Amazon Basin. *J. Geophys. Res.* **104**, 14189−14198.

Dirmeyer, P. A. & Brubaker, K. L. (1999) Contrasting evaporative moisture sources during the drought of 1988 and the flood of 1993. *J. Geophys. Res.* **104**(D16), 19383–19397.

Dirmeyer, P. A. & Brubaker, K. L. (2007) Characterization of the global hydrologic cycle from a back-trajectory analysis of atmospheric water vapor. *J. Hydromet.* **8**, 20–37.

Dominguez, F., Kumar, P., Liang, X. & Ting, M. (2006) Impact of atmospheric moisture storage on precipitation recycling. *J. Climate* **19**, 1513–1530.

Eltahir, E. A. B. & Bras, R. L. (1996) Precipitation recycling. *Rev. Geophys.* **34**, 367–378.

Fernández, J., Sáenz, J. & Zorita, E. (2003) Analysis of wintertime atmospheric moisture transport and its variability over southern Europe in the NCEP-Reanalyses. *Climate Res.* **23**, 195−215.

Hanna, S. R. (1982) Applications in air pollution modelling. In: *Atmospheric Turbulence and Air Pollution Modelling* (ed. by F. T. M. Nieuwstadt & H. van Dop), 275–310. Reidel, Dordrecht, The Netherlands.

Hastenrath, S. L. (1966) The flux of atmospheric water vapor over the Caribbean Sea and the Gulf of Mexico. *J. Appl. Met.* **5**, 778−788.

Hastenrath, S. (2002) The Intertropical Convergence Zone of the eastern Pacific revisited. *Int. J. Climatol*. **22**, 347–356.

Held, I. M. & Soden, B. J. (2006) Robust responses of the hydrological cycle to global warming. *J. Climate* **19**, 5686−5699.

Huffman, G. J., Adler, R. F., Morrissey, M. M., Curtis, S., Joyce, R., McGavock, B. & Susskind, J. (2001) Global precipitation at one-degree daily resolution from multi-satellite observations. *J. Hydromet.* **2**, 36–50.

IPCC (Intergovernmental Panel on Climate Change) (2007) Summary for Policymakers. In: *Climate Change 2007: The Physical Science Basis*. Contribution of Working Group I to the Fourth Assessment Report of the Intergovernmental Panel on Climate Change (ed. by S. Solomon, D. Qin, M. Manning, Z. Chen, M. Marquis, K. B. Averyt, M. Tignor. & H. L. Miller). Cambridge University Press, Cambridge, UK and New York, NY, USA (available at http://www.ipcc.ch/pdf/assessment-report/ar4/wg1/ar4-wg1-spm.pdf, last visited on 15 April 2008).

Joussame, S., Jouzel, J. & Sadourny, R. (1984) A general circulation model of water isotope cycles in the atmosphere. *Nature* **311**, 24–29.

Kalnay, E., Kanamitsu, M., Kistler, R., Collins, W., Deaven, D., Gandin, L., Iredell, M., Saha, S., White G., Woollen, J., Zhu, Y., Leetmaa, A., Reynolds, B., Chelliah, M., Ebisuzaki, W., Higgins, W., Janowiak, J., Mo, K.C., Ropelewski, C., Wang, J., Jenne, R. & Joseph, D. (1996) The NCEP/NCAR 40-year Reanalysis Project. *Bull. Am. Met. Soc*. **77**, 437–471.

Kistler, R., Kalnay, E., Collins, W., Saha, S., White, G., Woollen, J., Chelliah, M., Ebisuzaki, W., Kanamitsu, M., Kousky, V., Van den Dool, H., Jenne, R. & Fiorino, M. (2001) The NCEP–NCAR 50-year reanalysis: monthly means CD-ROM and documentation. *Bull. Am. Met. Soc.* **82**, 247–267.

Koster, R., Jouzel, J., Suozzo, R., Russell, G., Broecker, W., Rind, D. & Eagleson, P. (1986) Global sources of local precipitation as determined by the NASA/GISS GCM. *Geophys. Res. Lett.* **13**, 121−124.

Labraga, J.C., Frumento, O. & López, M. (2000) The atmospheric water vapor cycle in South America and the tropospheric circulation. *J. Climate* **13**, 1899−1915.

Liu, J. & Stewart, R. E. (2003) Water vapor fluxes over the Saskatchewan River basin. *J. Hydromet.* **4**, 944−959.

Marengo, J. A. & Nobre, C. A. (2001) The hydroclimatological framework in Amazonia. In: *Biogeochemistry of Amazonia* (ed. by J. Richey, M. McClaine & R. Victoria), 17−42. Oxford University Press, Oxford, UK.

Marengo, J. A. (2005) The characteristics and variability of the atmospheric water balance in the Amazon basin: spatial and temporal variability. *Climate Dynamics* **24**, 11−22.

Marengo, J. A. (2006) On the hydrological cycle of the Amazon Basin: a historical review and current state-of-the-art. *Revista Brasileira de Meteorologia* **21**(3), 1−19.

Massacand, A. C., Wernli, H. & Davies, H. C. (1998) Heavy precipitation on the Alpine southside: an upper-level precursor. *Geophys. Res. Lett.* **25**(9), 1435–1438.

Molion, L. C. B. (1975) A climatonomic study of the energy and moisture fluxes of the Amazon basin with considerations of deforestation effects. PhD Thesis, University of Wisconsin, Madison, USA.

Nieto, R., Gimeno, L. & Trigo, R. M. (2006) A Lagrangian identification of major sources of Sahel moisture. *Geophys. Res. Lett.* **33**(L18707), doi:10.1029/2006GL027232.

Nieto, R., Gimeno, L., Gallego, D. & Trigo, R. M. (2007) Contributions to the moisture budget of airmasses over Iceland. *Meteor. Zeits.* **6**(1), 1−3, doi:10.1127/0941-2948/2007/0176.

Numaguti, A. (1999) Origin and recycling processes of precipitating water over the Eurasian continent: experiments using an atmospheric general circulation model. *J. Geophys. Res.* **104**, 1957−1972.

Poveda, G., Waylen, P. R. & Pulwarty, R. S. (2006). Annual and inter-annual variability of the present climate in northern South America and southern Mesoamerica. *Palaeogeogr., Palaeoclim., Palaeoecol.* **234**, 3–27.

Rappenglueck, B., Forster, C., Jakobi, G., Pesch, M., Shallcross, D. E. & Fabian, P. (2004) On the occurrence of enhanced levels of PAN and ozone over Berlin, Germany. *Atmos. Env.* **38**, 6125−6134.

Rindsberger, M., Magaritz, M., Carmi, I. & Gilad, D. (1983) The relation between air mass trajectories and the water isotope composition in the Mediterranean Sea area. *Geophys. Rev. Lett.* **10**, 43−46.

Salati, E. & Marques, J. (1984) Climatology of the Amazon region. In: *The Amazon: Limnology and Landscape Ecology of a Mighty Tropical River and its Basin* (ed. by H. Sioli). W. Junk, Dordrecht, The Netherlands.

Silva León, G. (2005) La cuenca del río Orinoco: visión hidrográfica y balance hídrico (The Orinoco River basin: hydrographic view and its hydrological balance). *Revista Geografica Venezolana* **46**(1), 75−108.

Stohl, A., Hittenberger, M. & Wotawa, G. (1998) Validation of the Lagrangian particle dispersion model FLEXPART against large scale tracer experiment data. *Atmos. Environ.* **32**, 4245−4264.

Stohl, A. & Thompson, D. J. (1999) A density correction for Lagrangian particle dispersion models. *Bound.-Layer Met.* **90**, 155−167.

Stohl, A., Eckhardt, S., Foster, C., James, P. & Spichtinger, N. (2002) On the pathways and timescales of intercontinental air pollution transport. *J. Geophys. Res.* **107**, 4684, doi:10.1029/2001JD001396.

Stohl, A. & James, P. (2004) A Lagrangian analysis of the atmospheric branch of the global water cycle. Part I: Method description, validation and demonstration for the August 2002 flooding in Central Europe. *J. Hydromet.* **5**, 656−678.

Stohl, A. & James, P. (2005) A Lagrangian analysis of the atmospheric branch of the global water cycle. Part II: Moisture transports between Earth's ocean basins and river catchments. *J. Hydromet.* **6**, 961−984.

Trenberth, K. E., Dai, A., Rasmussen, R. M. & Parsons, D. B. (2003) The changing character of precipitation. *Bull. Am. Met. Soc.* **84**, 1205−1217.

Trenberth, K. E. & Guillemot, C. J. (1998) Evaluation of the atmospheric moisture and hydrological cycle in the NCEP/NCAR reanalysis. *Clim. Dyn.* **14**, 213–231.

USAID (2000) Venezuela Factsheet, February, 2000. USAID Office of Foreign Disaster Assistance.

Vogelezang, D. H. P. & Holtslag, A. A. M. (1996) Evaluation and model impacts of alternative boundary-layer height formulations. *Bound.-Layer Met.* **81**, 245−269.

Wernli, H. (1997) A Lagrangian-based analysis of extratropical cyclones. II: A detailed case-study, *Quart. J. Roy. Met. Soc.* **123**, 1677–1706.

Wernli, H., Dirren, S., Liniger, M. & Zillig, M. (2002) Dynamical aspects of the life cycle of the winter storm "Lothar" (24–26 December 1999). *Quart. J. Roy. Met. Soc.* **128**(580), 405–429.

ECMWF (European Center for Medium-range Weather Forecasting) (2002) IFS documentation. ECMWF REP, Reading, UK. Available at: http://www.ecmwf.int.

Wright, W. E., Long, A., Comrie, A. C., Leavitt, S. W., Cavazos, T. & Eastoe, C. (2001) Monsoonal moisture sources revealed using temperature, precipitation and precipitation stable isotope timeseries. *Geophys. Res. Lett.* **28**, 787–790.

Received 31 May 2007; accepted 22 February 2008